Bounds on the $Z\gamma\gamma$ couplings from HERA

F. Cornet[a], R. Graciani[b], J.I. Illana[a]

[a] Depto. de Física Teórica y del Cosmos, Universidad de Granada, E-18071 Granada, Spain
[b] Depto. de Física Teórica, Universidad Autónoma de Madrid, E-28049 Cantoblanco, Spain

Abstract: The possibility of testing trilinear neutral gauge boson couplings in radiative neutral current scattering at HERA is analyzed using a Monte Carlo program that includes the Standard Model at tree level and the anomalous vertices. Acceptance and isolation cuts are applied as well as optimized cuts to enhance the signal from new physics. The bounds on $Z\gamma\gamma$ couplings that can be achieved are not so stringent as present bounds, even for high luminosities, but probe a different kinematical region almost unsensitive to form factors.

1 Introduction

The precision data collected to date have confirmed the Standard Model to be a good description of physics below the electroweak scale [1]. Despite of its great success, there are many reasons to believe that some kind of new physics must exist. On the other hand, the non-abelian structure of the gauge boson self-couplings is still poorly tested and one of the most sensitive probes for new physics is provided by the trilinear gauge boson couplings (TGC) [2].

Many studies have been devoted to the $WW\gamma$ and WWZ couplings. At hadron colliders and e^+e^- colliders, the present bounds (Tevatron [3]) and prospects (LHC, LEP2 and NLC [2, 4]) are mostly based on diboson production (WW, $W\gamma$ and WZ). In ep collisions, HERA could provide further information analyzing single W production ($ep \to eWX$ [5]) and radiative charged current scattering ($ep \to \nu\gamma X$ [6]). There is also some literature on $WW\gamma$ couplings in W-pair production at future very high energy photon colliders (bremsstrahlung photons in peripheral heavy ion collisions [7] and Compton backscattered laser beams [8]).

Only recently, attention has been paid to the $Z\gamma Z$, $Z\gamma\gamma$ and ZZZ couplings. There is a detailed analysis of $Z\gamma V$ couplings ($V = \gamma, Z$) for hadron colliders in [9]. CDF [10] and DØ [11] have obtained bounds on the $Z\gamma Z$ and $Z\gamma\gamma$ anomalous couplings, while L3 has studied only the first ones [12]. Studies on the sensitivities to these vertices in future e^+e^- colliders, LEP2 [4] and NLC [13], have been performed during the last years. Some proposals have been made to probe these neutral boson gauge couplings at future photon colliders in $e\gamma \to Ze$ [14].

In this work we study the prospects for measuring the TGC in the process $ep \to e\gamma X$. In particular, we will concentrate on the $Z\gamma\gamma$ couplings, which can be more stringently bounded than the $Z\gamma Z$ ones for this process.

In Section 2, we present the TGC. The next section deals with the different contributions to the process $ep \to e\gamma X$ and the cuts and methods we have employed in our analysis. Section 4 contains our results for the Standard Model total cross section and distributions and the estimates of the sensitivity of these quantities to the presence of anomalous couplings. Finally, in the last section we present our conclusions.

2 Phenomenological parametrization of the neutral TGC

A convenient way to study deviations from the standard model predictions consists of considering the most general lagrangian compatible with Lorentz invariance, the electromagnetic U(1) gauge symmetry, and other possible gauge symmetries.

For the trilinear $Z\gamma V$ couplings ($V = \gamma, Z$) the most general vertex function invariant under Lorentz and electromagnetic gauge transformations can be described in terms of four independent dimensionless form factors [15], denoted by h_i^V, i=1,2,3,4:

$$\Gamma^{\alpha\beta\mu}_{Z\gamma V}(q_1, q_2, p) = \frac{f(V)}{M_Z^2}\{h_1^V(q_2^\mu g^{\alpha\beta} - q_2^\alpha g^{\mu\beta}) + \frac{h_2^V}{M_Z^2}p^\alpha(p\cdot q_2 g^{\mu\beta} - q_2^\mu p^\beta) + h_3^V \varepsilon^{\mu\alpha\beta\rho} q_{2_\rho} + \frac{h_4^V}{M_Z^2} p^\alpha \varepsilon^{\mu\beta\rho\sigma} p_\rho q_{2_\sigma}\}. \quad (1)$$

Terms proportional to p^μ, q_1^α and q_2^β are omitted as long as the scalar components of all three vector bosons can be neglected (whenever they couple to almost massless fermions) or they are zero (on-shell condition for Z or U(1) gauge boson character of the photon). The overall factor, $f(V)$, is $p^2 - q_1^2$ for $Z\gamma Z$ or p^2 for $Z\gamma\gamma$ and is a result of Bose symmetry and electromagnetic gauge invariance. These latter constraints reduce the familiar seven form factors of the most general WWV vertex to only these four for the $Z\gamma V$ vertex. There still remains a global factor that can be fixed, without loss of generality, to $g_{Z\gamma Z} = g_{Z\gamma\gamma} = e$. Combinations of $h_3^V(h_1^V)$ and $h_4^V(h_2^V)$ correspond to electric (magnetic) dipole and magnetic (electric) quadrupole transition moments in the static limit.

All the terms are C-odd. The terms proportional to h_1^V and h_2^V are CP-odd while the other two are CP-even. All the form factors are zero at tree level in the Standard Model. At the one-loop level, only the CP-conserving h_3^V and h_4^V are nonzero [16] but too small ($\mathcal{O}(\alpha/\pi)$) to lead to any observable effect at any present or planned experiment. However, larger effects might appear in theories or models beyond the Standard Model, for instance when the gauge bosons are composite objects [17].

This is a purely phenomenological, model independent parametrization. Tree-level unitarity restricts the $Z\gamma V$ to the Standard Model values at asympotically high energies [18]. This implies that the couplings h_i^V have to be described by form factors $h_i^V(q_1^2, q_2^2, p^2)$ which vanish when q_1^2, q_2^2 or p^2 become large. In hadron colliders, large values of $p^2 = \hat{s}$ come into play and the energy dependence has to be taken into account, including unknown dumping factors [9]. A scale dependence appears as an additional parameter (the scale of new physics, Λ). Alternatively, one could introduce a set of operators invariant under SU(2)×U(1) involving the gauge bosons and/or additional would-be-Goldstone bosons and the physical Higgs. Depending on the new physics dynamics, operators with dimension d could be generated at the scale Λ, with a strength which is generally suppressed by factors like $(M_W/\Lambda)^{d-4}$ or $(\sqrt{s}/\Lambda)^{d-4}$ [19]. It can be shown

that h_1^V and h_3^V receive contributions from operators of dimension ≥ 6 and h_2^V and h_4^V from operators of dimension ≥ 8. Unlike hadron colliders, in $ep \to e\gamma X$ at HERA energies, we can ignore the dependence of the form factors on the scale. On the other hand, the anomalous couplings are tested in a different kinematical region, which makes their study in this process complementary to the ones performed at hadron and lepton colliders.

3 The process $ep \to e\gamma X$

The process under study is $ep \to e\gamma X$, which is described in the parton model by the radiative neutral current electron-quark and electron-antiquark scattering,

$$e^- \overset{(-)}{q} \to e^- \overset{(-)}{q} \gamma. \tag{2}$$

There are eight Feynman diagrams contributing to this process in the Standard Model and three additional ones if one includes anomalous vertices: one extra diagram for the $Z\gamma Z$ vertex and two for the $Z\gamma\gamma$ vertex (Fig. 1).

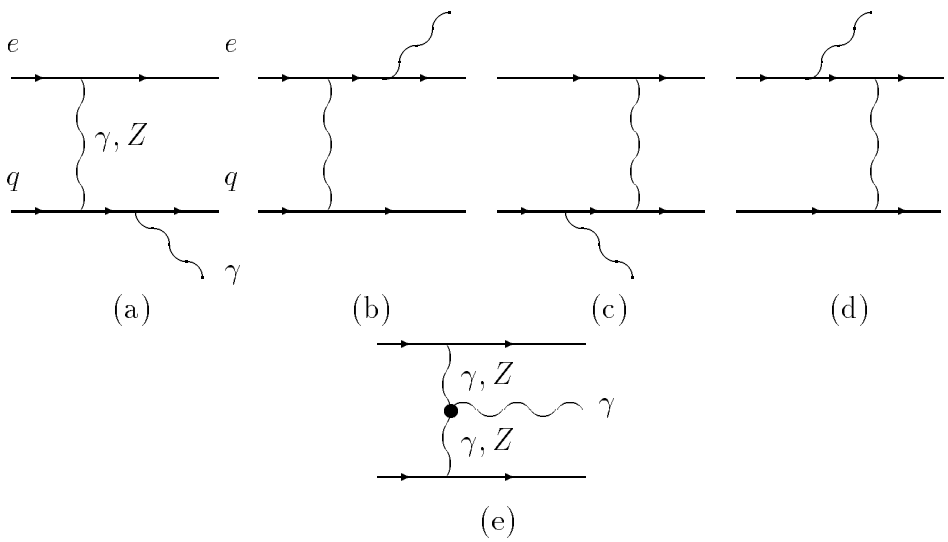

Figure 1: *Feynman diagrams for the process* $e^-q \to e^-q\gamma$.

Diagrams with γ exchanged in the t-channel are dominant. Nevertheless, we consider the whole set of diagrams in the calculation. On the other side, u-channel fermion exchange poles appear, in the limit of massless quarks and electrons (diagrams (c) and (d)). Since the anomalous diagrams (e) do not present such infrared or collinear singularities, it seems appropriate to avoid almost on-shell photons exchanged and fermion poles by cutting the transverse momenta of the final fermions (electron and jet) to enhance the signal from anomalous vertices. Due to the suppression factor coming from Z propagator, the anomalous diagrams are more sensitive to $Z\gamma\gamma$ than to $Z\gamma Z$ vertices. In the following we will focus our attention on the former.

The basic variables of the parton level process are five. A suitable choice is: E_γ (energy of the final photon), $\cos\theta_\gamma$, $\cos\theta_{q'}$ (cosines of the polar angles of the photon and the scattered quark

defined with respect to the proton direction), ϕ (the angle between the transverse momenta of the photon and the scattered quark in a plane perpendicular to the beam), and a trivial azimuthal angle that is integrated out (unpolarized beams). All the variables are referred to the laboratory frame. One needs an extra variable, the Bjorken-x, to connect the partonic process with the ep process. The phase space integration over these six variables is carried out by `VEGAS` [20] and has been cross-checked with the `RAMBO` subroutine [21].

We adopt two kinds of event cuts to constrain conveniently the phase space:

- *Acceptance and isolation* cuts. The former are to exclude phase space regions which are not accessible to the detector, because of angular or efficiency limitations:[1]

$$\begin{aligned} 8^o < \theta_e,\ \theta_\gamma,\ \theta_{\rm jet} < 172^o; \\ E_e,\ E_\gamma,\ p_{\rm T}^{\rm q'} > 10\ {\rm GeV}. \end{aligned} \tag{3}$$

  The latter keep the final photon well separated from both the final electron and the jet:

$$\begin{aligned} \cos\langle\gamma, e\rangle < 0.9; \\ R > 1.5, \end{aligned} \tag{4}$$

  where $R \equiv \sqrt{\Delta\eta^2 + \phi^2}$ is the separation between the photon and the jet in the rapidity-azimuthal plane, and $\langle\gamma, e\rangle$ is the angle between the photon and the scattered electron.

- Cuts for *intrinsic background suppression*. They consist of strengthening some of the previous cuts or adding new ones to enhance the signal of the anomalous diagrams against the Standard Model background.

We have developed a Monte Carlo program for the simulation of the process $ep \to e\gamma X$ where X is the remnant of the proton plus one jet formed by the scattered quark of the subprocess (2). It includes the Standard Model helicitity amplitudes computed using the `HELAS` subroutines [22]. We added new code to account for the anomalous diagrams. The squares of these anomalous amplitudes have been cross-checked with their analytical expressions computed using `FORM` [23]. For the parton distribution functions, we employ both the set 1 of Duke-Owens' parametrizations [25] and the modified MRS(A) parametrizations [26], with the scale chosen to be the hadronic momentum transfer.

As inputs, we use the beam energies $E_e = 30$ GeV and $E_p = 820$ GeV, the Z mass $M_Z = 91.187$ GeV, the weak angle $\sin^2_W = 0.2315$ [24] and the fine structure constant $\alpha = 1/128$. A more correct choice would be the running fine structure constant with Q^2 as the argument. However, as we are interested in large Q^2 events, the value $\alpha(M_Z^2)$ is accurate enough for our purposes. We consider only the first and second generations of quarks, assumed to be massless.

We start by applying the cuts (3) and (4) and examining the contribution to a set of observables of the Standard Model and the anomalous diagrams, separately. Next, we select one observable such that, when a cut on it is performed, only Standard Model events are mostly eliminated. The procedure is repeated with this new cut built in. After several runs, adding new cuts, the ratio standard/anomalous cross sections is reduced and hence the sensitivity to anomalous couplings is improved.

[1] The threshold for the transverse momentum of the scattered quark ensures that its kinematics can be described in terms of a jet.

4 Results

4.1 Observables

The total cross section of $ep \to e\gamma X$ can be written as

$$\sigma = \sigma_{\rm SM} + \sum_i \tau_i \cdot h_i^\gamma + \sum_i \sigma_i \cdot (h_i^\gamma)^2 + \sigma_{12} \cdot h_1^\gamma h_2^\gamma + \sigma_{34} \cdot h_3^\gamma h_4^\gamma. \tag{5}$$

The forthcoming results are obtained using the MRS'95 parametrization of the parton densities[2] [26]. The linear terms of the P-violating couplings h_3^γ and h_4^γ are negligible, as they mostly arise from the interference of standard model diagrams with photon exchange (P-even) and anomalous P-odd diagrams ($\tau_3 \simeq \tau_4 \simeq 0$). Moreover, anomalous diagrams with different P do not interfere either. On the other hand, the quadratic terms proportional to $(h_1^\gamma)^2$ and $(h_3^\gamma)^2$ have identical expressions, and the same for h_2^γ and h_4^γ ($\sigma_1 = \sigma_3$, $\sigma_2 = \sigma_4$). Only the linear terms make their bounds different. The interference terms σ_{12} and σ_{34} are also identical.

We have analyzed the distributions of more than twenty observables in the laboratory frame, including the energies, transverse momenta and angular distributions of the jet, the photon and the final electron, as well as their spatial, polar and azimuthal separations. Also the bjorken-x, the leptonic and hadronic momenta transfer and other fractional energies are considered.

The process of intrinsic background suppression is illustrated by comparing Figures 2 and 3. For simplicity, only the most interesting variables are shown: the energy $E(\gamma)$ and transverse momentum $p_T(\gamma)$ of the photon; the angles between the photon and the scattered electron $\langle \gamma, e \rangle$, the photon and the jet $\langle \gamma, j \rangle$, and the scattered electron and the jet $\langle e, j \rangle$; and the leptonic momentum transfer $Q^2(e)$. In Fig. 2, these variables are plotted with only acceptance and isolation cuts implemented. All of them share the property of disposing of a range where any anomalous effect is negligible, whereas the contribution to the total SM cross section is large. The set of cuts listed below were added to reach eventually the distributions of Fig. 3:

- The main contribution to the Standard Model cross section comes from soft photons with very low transverse momentum. The following cuts suppress a 97% of these events, without hardly affecting the anomalous diagrams which, conversely, enfavour high energy photons:

$$\begin{aligned} E_\gamma &> 30 \text{ GeV} \\ p_T^\gamma &> 20 \text{ GeV} \end{aligned} \tag{6}$$

- Another remarkable feature of anomalous diagrams is the very different typical momentum transfers. Let's concentrate on the leptonic momentum transfer, $Q_e^2 = -(p'_e - p_e)^2$. The phase space enhances high Q_e^2, while the photon propagator of the Standard Model diagrams prefer low values (above the threshold for electron detectability, $Q_e^2 > 5.8$ GeV^2, with our required minimum energy and angle). On the contrary, the anomalous diagrams have always a Z propagator which introduces a suppression factor of the order of Q_e^2/M_Z^2 and makes irrelevant the Q_e^2 dependence, which is only determined by the phase space. As a consequence, the following cut looks appropriate,

$$Q_e^2 > 1000 \text{ GeV}^2 \tag{7}$$

[2] The values change $\sim 10\%$ when using the (old) Duke-Owens' structure functions.

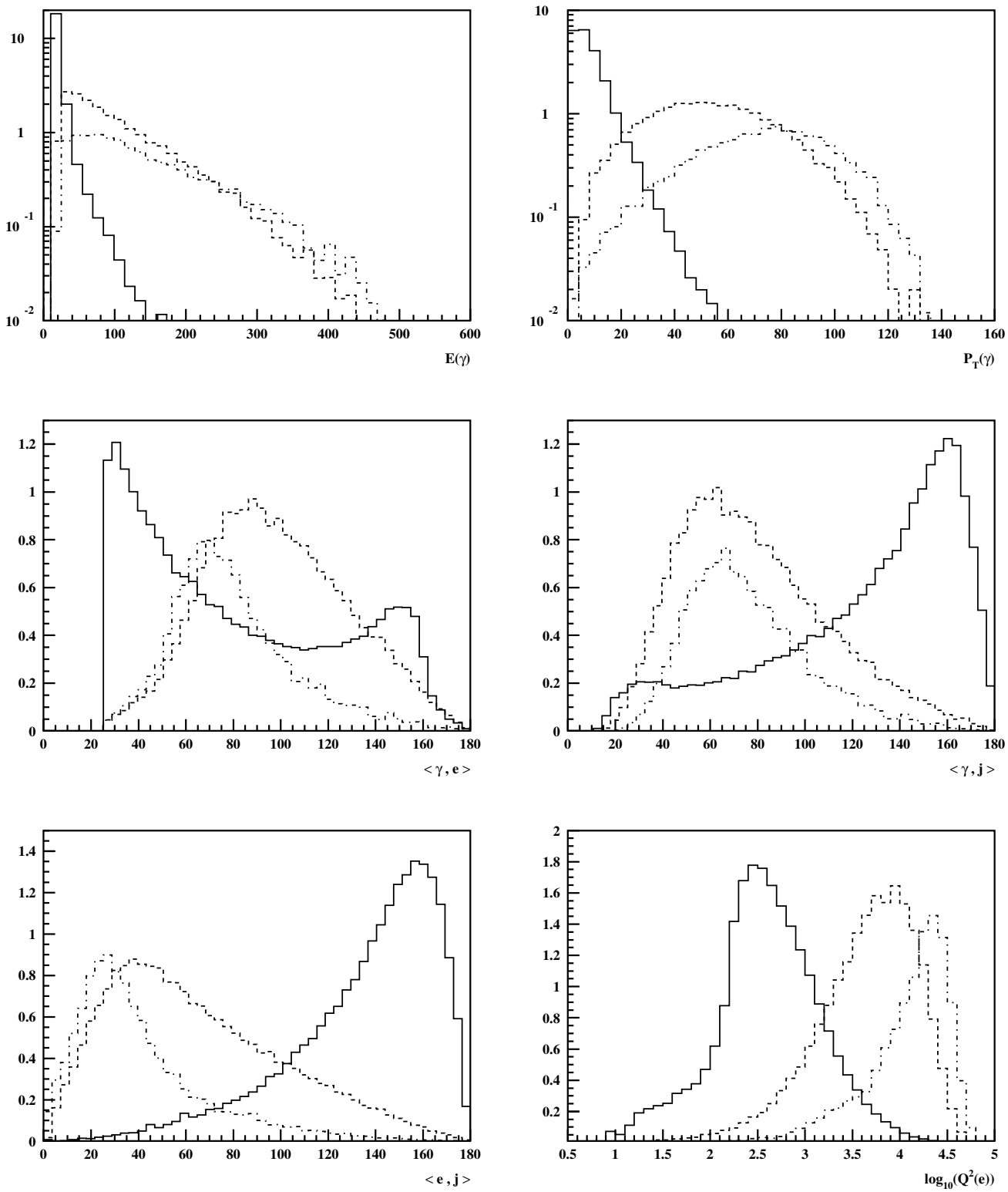

Figure 2: *Differential cross sections (pb) for the process* $ep \to e\gamma X$ *at HERA, with only acceptance and isolation cuts. The solid line is the Standard Model contribution and the dash (dot-dash) line correspond to 10000 times the* σ_1 *(*σ_2*) anomalous contributions.*

It is important to notice at this point why usual form factors for the anomalous couplings can be neglected at HERA. For our process, these form factors should be proportional to $1/(1 + Q^2/\Lambda^2)^n$. With the scale of new physics $\Lambda = 500$ GeV to 1 TeV, these factors can

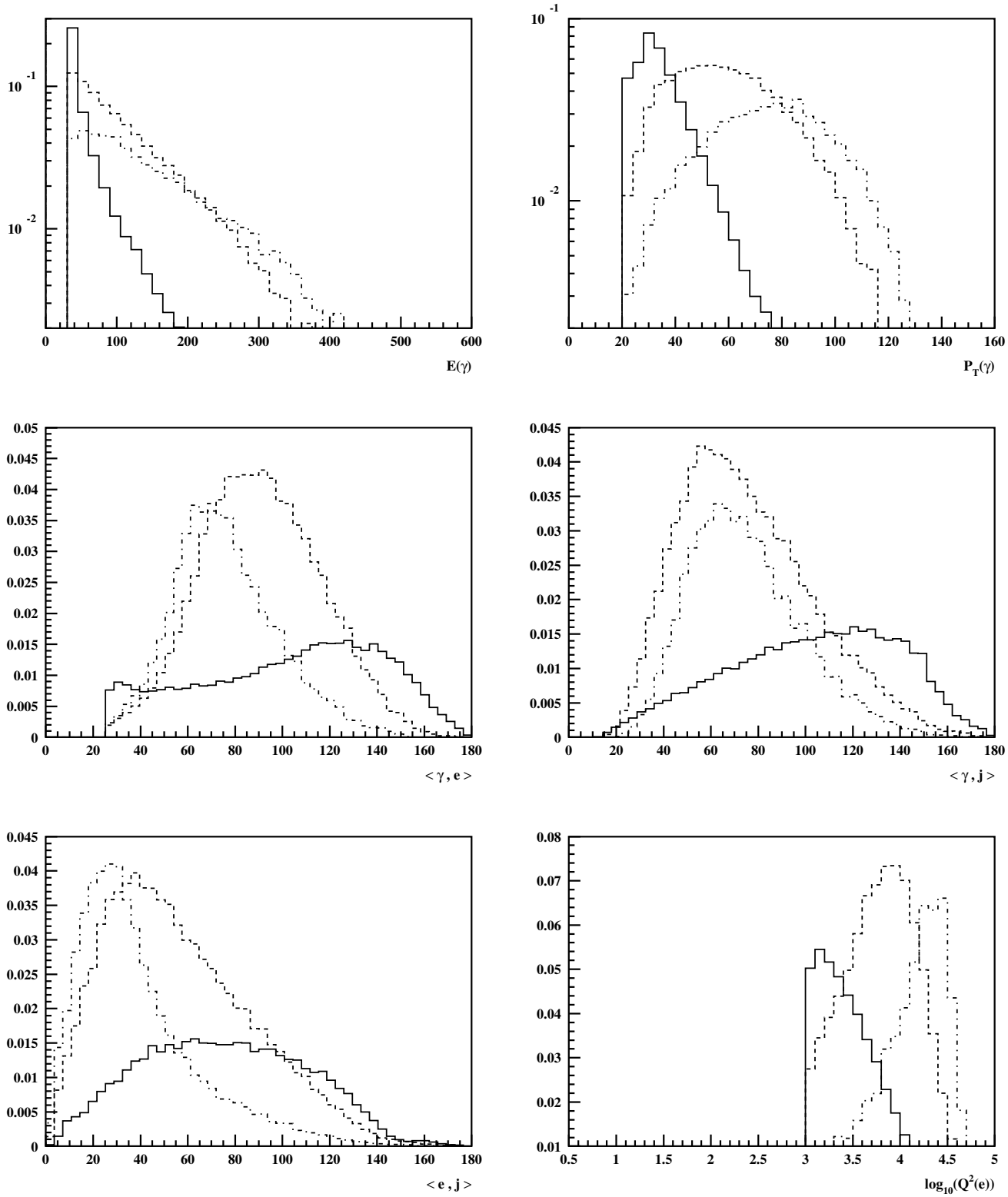

Figure 3: *Differential cross sections (pb) for the process* $ep \to e\gamma X$ *at HERA, after intrinsic background suppression. The solid line is the Standard Model contribution and the dash (dot-dash) line correspond to 500 times the* σ_1 *(*σ_2*) anomalous contributions.*

be taken to be one. This is not the case in lepton or hadron high energy colliders where the diboson production in the s-channel needs dumping factors $1/(1+\hat{s}/\Lambda^2)^n$.

The total cross section for the Standard Model with acceptance and isolation cuts is $\sigma_{\rm SM} = 21.38$ pb and is reduced to 0.37 pb when all the cuts are applied, while the quadratic contributions only change from $\sigma_1 = 2 \times 10^{-3}$ pb, $\sigma_2 = 1.12 \times 10^{-3}$ pb to $\sigma_1 = 1.58 \times 10^{-3}$ pb, $\sigma_2 = 1.05 \times 10^{-3}$ pb. The linear terms are of importance and change from $\tau_1 = 1.18 \times 10^{-2}$ pb, $\tau_2 = 1.27 \times 10^{-3}$ pb to $\tau_1 = 7.13 \times 10^{-3}$ pb, $\tau_2 = 1.26 \times 10^{-3}$ pb. Finally, the interference term $\sigma_{12} = 1.87 \times 10^{-3}$ pb changes to $\sigma_{12} = 1.71 \times 10^{-3}$ pb.

The typical Standard Model events consist of soft and low-p_T photons mostly backwards, tending to go in the same direction of the scattered electrons (part of them are emitted by the hadronic current in the forward direction), close to the required angular separation ($\sim 30^o$). The low-p_T jet goes opposite to both the photon and the scattered electron, also in the transverse plane. On the contrary, the anomalous events have not so soft and high-p_T photons, concentrated in the forward region as it the case for the scattered electron and the jet.

4.2 Sensitivity to anomalous couplings

In order to estimate the sensitivity to anomalous couplings, we consider the χ^2 function. One can define the χ^2, which is related to the likelihood function $\mathcal{L}$, as

$$\chi^2 \equiv -2 \ln \mathcal{L} = 2L \left(\sigma^{th} - \sigma^o + \sigma^o \ln \frac{\sigma^o}{\sigma^{th}} \right) \simeq L \frac{(\sigma^{th} - \sigma^o)^2}{\sigma^o}, \tag{8}$$

where $L = N^{th}/\sigma^{th} = N^o/\sigma^o$ is the integrated luminosity and N^{th} (N^o) is the number of theoretical (observed) events. The last line of (8) is a useful and familiar approximation, only valid when $\mid \sigma^{th} - \sigma^o \mid /\sigma^o \ll 1$. This function is a measure of the probability that statistical fluctuations can make undistinguisable the observed and the predicted number of events, that is the Standard Model prediction. The well known χ^2-CL curve allows us to determine the corresponding confidence level (CL). We establish bounds on the anomalous couplings by fixing a certain $\chi^2 = \delta^2$ and allowing for the h_i^γ values to vary, $N^o = N^o(h_i^\gamma)$. The parameter δ is often referred as the number of standard deviations or 'sigmas'. A 95% CL corresponds to almost two sigmas ($\delta = 1.96$). When $\sigma \simeq \sigma_{\rm SM} + (h_i^\gamma)^2 \sigma_i$ (case of the CP-odd terms) and the anomalous contribution is small enough, the upper limits present some useful, approximate scaling properties, with the luminosity,

$$h_i^\gamma(L') \simeq \sqrt[4]{\frac{L}{L'}}\, h_i^\gamma(L). \tag{9}$$

A brief comment on the interpretation of the results is in order. As the cross section grows with h_i^γ, in the relevant range of values, the N^o upper limits can be regarded as the lowest number of measured events that would discard the Standard Model, or the largest values of h_i^γ that could be bounded if no effect is observed, with the given CL. This procedure approaches the method of upper limits for Poisson processes when the number of events is large ($\gtrsim 10$).

In Fig. 4 the sensitivities for different luminosities are shown. Unfortunately, HERA cannot compete with Tevatron, whose best bounds, reported by the DØ collaboration [11], are

$$\begin{aligned} |h_1^\gamma|,\ |h_3^\gamma| &< 1.9\ (3.1), \\ |h_2^\gamma|,\ |h_4^\gamma| &< 0.5\ (0.8). \end{aligned} \tag{10}$$

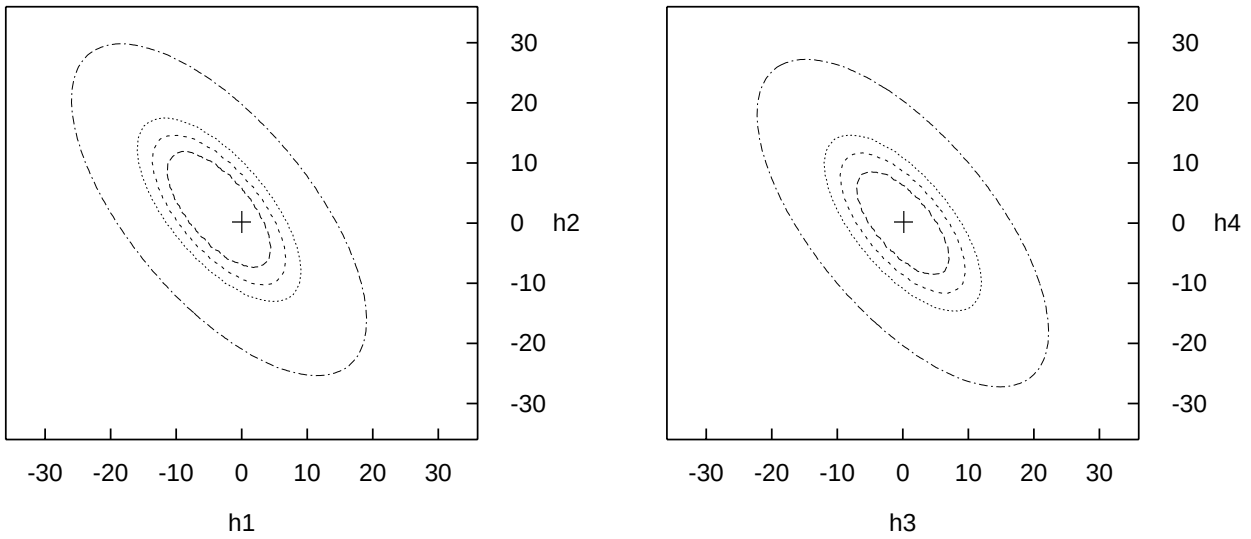

Figure 4: *Limit contours for $Z\gamma\gamma$ couplings at HERA with an integrated luminosity of 10, 100, 250, 1000 pb^{-1} and a 95% CL.*

HERA	10 pb^{-1}		100 pb^{-1}		250 pb^{-1}		1 fb^{-1}	
h_1^γ	-19.0	14.5	-11.5	7.0	-9.5	5.5	-8.0	3.5
	-26.0	19.5	-16.0	9.5	-14.0	7.0	-11.5	4.5
h_2^γ	-21.5	20.0	-12.0	10.0	- 9.5	8.0	-7.0	6.0
	-26.0	30.0	-13.0	18.0	-10.0	15.0	- 7.5	12.0
h_3^γ	-17.0	17.0	-9.0	9.0	-7.5	7.5	-5.5	5.5
	-22.5	22.5	-12.0	12.0	-10.0	10.0	-7.0	7.0
h_4^γ	-20.5	20.5	-11.0	11.0	-8.5	8.5	-6.0	6.0
	-27.5	27.5	-14.5	14.5	-12.0	12.0	-8.5	8.5

Table 1: *Axial and correlated limits for the $Z\gamma\gamma$ anomalous couplings at HERA with different integrated luminosities and 95% CL.*

For the first value it was assumed that only one anomalous coupling contributes ('axial limits') and for the second there are two couplings contributing ('correlated limits'). Our results are summarized in Table 1.

The origin of so poor results is the fact that, unlike diboson production at hadron or e^+e^- colliders, the anomalous diagrams of $ep \to e\gamma X$ have a Z propagator decreasing their effect. The process $ep \to eZX$ avoids this problem thanks to the absence of these propagators: the Standard Model cross section is similar to the anomalous one but, as a drawback, they are of the order of femtobarns.

5 Summary and conclusions

The radiative neutral current process $ep \to e\gamma X$ at HERA has been studied. Realistic cuts have been applied in order to observe a clean signal consisting of detectable and well separated electron, photon and jet.

The possibility of testing the trilinear neutral gauge boson couplings in this process has also been explored. The $Z\gamma Z$ couplings are very suppressed by two Z propagators. Only the $Z\gamma\gamma$ couplings have been considered. A Monte Carlo program has been developed to account for such anomalous vertex and further cuts have been implemented to improve the sensitivity to this source of new physics. Our estimates are based on total cross sections since the expected number of events is so small that a distribution analysis is not possible. The distributions just helped us to find the optimum cuts. Unfortunately, competitive bounds on these anomalous couplings cannot be achieved at HERA, even with the future luminosity upgrades.[3] As a counterpart, a different kinematical region is explored, in which the form factors can be neglected.

Acknowledgements

One of us (J.I.) would like to thank the Workshop organizers for financial support and very especially the electroweak working group conveners and the Group from Madrid at ZEUS for hospitality and useful conversations. This work has been partially supported by the CICYT and the European Commission under contract CHRX-CT-92-0004.

References

[1] D. Schaile: in *Proceedings of the 27th International Conference on High Energy Physics*, Glasgow, Scotland, 1994, edited by P.J. Bussey and I.G. Knowles (IOP, London, 1995), p. 27.

[2] H. Aihara et al.: FERMILAB-PUB-95/031, to be published in "Electroweak Symmetry Breaking and Beyond the Standard Model", eds. T. Barklow, S. Dawson, H. Haber and J. Seigrist.

[3] S.M. Errede: in *Proc. of the 27th International Conference on High Energy Physics*, Glasgow, Scotland, 1994, edited by P.J. Bussey and I.G. Knowles (IOP, London, 1995), p. 433.

[4] G. Gounaris, J.-L. Kneur and D. Zeppenfeld: in *Report of the Workshop on Physics at LEP2*, CERN 96-01, p. 525.

[5] V. Noyes et al.: in these Proceedings.

[6] T. Helbig and H. Spiesberger: *Nucl. Phys.* **B373** (1992) 73.

[7] F. Cornet and J.I. Illana: *Phys. Rev. Lett.* **67** (1991) 1705.

[3] We would like to apologize for the optimistic but incorrect results that were presented at the workshop due to a regrettable and unlucky mistake in our programs.

[8] F.T. Brandt et al.: *Phys. Rev.* **D50** (1994) 5591;
S.Y. Choi and F. Schrempp: in *Proc. of the Workshop on e^+e^- collisions at 500 GeV: The Physics Potential*, Munich, Annecy, Hamburg, 1991, edited by P. Zerwas, DESY 92-123B (Hamburg, 1992), p. 795.

[9] U. Baur and E.L. Berger: *Phys. Rev.* **D47** (1993) 4889.

[10] F. Abe et al.: *Phys. Rev. Lett.* **74** (1995) 1941.

[11] S. Abachi et al.: *Phys. Rev. Lett.* **75** (1995) 1028.

[12] M. Aciarri et al.: *Phys. Lett.* **B346** (1995) 190.

[13] F. Boudjema et al.: *Phys. Rev.* **D43** (1991) 3683;
F. Boudjema: in *Proc. of the Workshop on e^+e^- collisions at 500 GeV: The Physics Potential*, Munich, Annecy, Hamburg, 1991, edited by P. Zerwas, DESY 93-123B (Hamburg, 1993), p. 757.

[14] F. Cornet: in *Proc. of the Workshop on e^+e^- collisions at 500 GeV: The Physics Potential*, Munnich, Annecy, Hamburg, 1991, edited by P. Zerwas, DESY 93-123C (Hamburg, 1993), p. 229;
S.Y. Choi: *Z. Phys.* **C68** (1995) 163.

[15] K. Hagiwara et al.: *Nucl. Phys.* **B282** (1987) 253.

[16] A. Barroso et al: *Z. Phys.* **C28** (1985) 149.

[17] M. Suzuki: *Phys. Lett.* **B153** (1985) 289;
T.G. Rizzo and M.A. Samuel: *Phys. Rev.* **D35** (1987) 403.

[18] J.M. Cornwall, D.N. Levin and G. Tiktopoulos: *Phys. Rev. Lett.* **30** (1973) 1268; *Phys. Rev.* **D10** (1974) 1145;
C.H. Lewellyn Smith: *Phys. Lett.* **46B** (1971) 233.

[19] G.J. Gounaris, F.M. Renard and G. Tsirogoti: *Phys. Lett.* **B338** (1994) 51; *Phys. Lett.* **B350** (1995) 212.

[20] G.P. Lepage: *Jour. Comp. Phys.* **27** (1978) 192.

[21] S.D. Ellis, R. Kleiss and W.J. Stirling: *RAMBO* fortran subroutine for phase space generation.

[22] H. Murayama, I. Watanabe and K. Hagiwara: *HELAS: HELicity Amplitude Subroutines for Feynman Diagram Evaluations*, KEK Report 91-11, January 1992;
T. Stelzer and W.F. Long: *Comput. Phys. Commun.* **81** (1994) 357.

[23] J. Vermaseren: *FORM User's Guide*, Nikhef Amsterdam, 1990.

[24] Particle Data Group: *Phys. Rev.* **D54** (1996) 1.

[25] D.W. Duke, J.F. Owens: *Phys. Rev.* **D30** (1984) 45.

[26] A.D. Martin, R.G. Roberts, W.J. Stirling: *Phys. Rev.* **D51** (1995) 4756.